Received: 21 October 2021 | Revised: 7 December 2021 | Accepted: 27 December 2021

DOI: 10.1002/app.52120

ARTICLE

Applied Polymer SCIENCE WILEY

Catalyst-free reprocessable crosslinked biobased polybenzoxazine-polyurethane based on dynamic carbamate chemistry

Zhibin Wen[1,2] | Leïla Bonnaud[2] | Philippe Dubois[2] | Jean-Marie Raquez[2]

[1]Shenzhen Institute of Advanced Electronic Materials, Shenzhen Institutes of Advanced Technology, Chinese Academy of Sciences, Shenzhen, China

[2]Laboratory of Polymeric and Composite Materials Center of Innovation and Research in Materials and Polymers, Materia Nova Research Center & University of Mons, Mons, Belgium

Correspondence
Zhibin Wen, Leïla Bonnaud, and Jean-Marie Raquez, Laboratory of Polymeric and Composite Materials Center of Innovation and Research in Materials and Polymers, Materia Nova Research Center & University of Mons, 23 Place du Parc, B-7000 Mons, Belgium.
Email: zhibin_wen@hotmail.com, jean-marie.raquez@umons.ac.be, and leila.bonnaud@materianova.be

Abstract

The introduction of dynamic covalent chemistry into the field of polymer chemistry has resulted in a new class of network polymer materials named covalent adaptable networks (CANs). These new materials have effectively bridged two antagonistic materials, that is, conventional thermoplastic and thermoset polymers together, thanks to these dynamic exchangeable covalent bonds, making them recyclable. In this work, we report a catalyst-free reprocessable polybenzoxazine-polyurethane thermosetting system with activation of carbamate dynamic bond exchange. The curing characteristics and properties of this biobased polybenzoxazine-polyurethane network have been determined by Fourier transform infra-red (FTIR), differential scanning calorimetry (DSC) and dynamic mechanical thermal analysis (DMA). Moreover, the tests of the recyclability of the material were successfully achieved under mild reprocess conditions (130°C, 10 min) thanks to the formation of abundant free phenolic hydroxyl groups. This work provides a promising potential for industrial applications as a new recyclable and reprocessable thermosetting polybenzoxazine material.

KEYWORDS

biopolymers and renewable polymers, polyurethane, thermosets

1 | INTRODUCTION

Polybenzoxazines have gained intense interest from academia and industry for the past few decades due to their good mechanical and thermal properties, excellent chemical resistance, low water uptake, and near-zero shrinkage. These unique characteristics make these materials have a wide range of applications in the fields of aerospace, electronic packaging and transportation.[1–3]

Polybenzoxazines are obtained through a ring-opening polymerization process of heterocyclic six-membered 1,3-benzoxazine monomer most commonly synthesized by a Mannich-like condensation of a phenol, a primary amine and formaldehyde.[3,4] The design flexibility results in the number of novel synthesized monomers constantly increasing. Nowadays, the number of renewable or sustainable phenolic or amine derivatives to replace the petroleum-based ones as well as the development of environmentally compatible and sustainable polymers have attracted considerable attention. In recent years, a large number of renewable phenol derivatives such as cardanol,[5,6] vanillin,[7,8] eugenol,[9–11] chavicol,[12] guaiacol,[13] sesamol,[14] umbelliferone,[15] arbutin,[16] urushiol,[17] catechol,[18] para-coumaric acid,[19] tyrosol,[20] and so forth have been chosen as the naturally occurring materials for benzoxazine precursors synthesis.

To obtain high thermal stability and modulus, highly crosslinked biobased polybenzoxazine thermosets have been widely reported. However, thermosetting materials also present major issues such as the inability to recycle, reshape, and reprocess. To address these drawbacks, covalent adaptable networks (CANs),[21–23] polymer networks with dynamic covalent bond exchange, bridge the stiffness of thermosets and the processability of thermoplastics into a single system. Several thermally activated dynamic covalent chemistries successfully enable dynamic exchange behavior in a variety of networks. These chemistries include Diels-Alder,[24,25] disulfide,[26] transesterification,[27,28] transcarbamoylation,[29–31] transthiocarbamoylation,[32–34] and so forth.

Different strategies have been employed in polybenzoxazines by Yagci et al. to achieve reprocessable properties. Such as sulfide linkages[35] or metal–ligand interactions.[36] Recently, Verge et al. reported a reversible catalyst-free polybenzoxazine vitrimer based on transesterification exchanges.[37] Expanding the scope of dynamic linkages, thermosetting polyurethanes are widely used in adhesives, foams, and coatings.[38] Traditionally, the dissociative reversion of carbamates typically occurred at high temperatures (>200°C).[39] In our previous work, the reversible addition reaction of the carbamate bond has been directly determined by real-time FTIR by monitoring the formation of isocyanates.[40] However, catalysts are usually required to active the dynamic bond exchange at appropriate temperature. Fortman et al. reported a catalyst-free polyhydroxyurethane vitrimer, showing excellent stress relaxation and repairability with the nucleophilic addition of free hydroxyl groups to the carbamate linkages.[31]

Interestingly, the ring-opening polymerization of benzoxazine precursors usually generates abundant free phenolic hydroxyl groups. In addition, the commercial availability of numerous hydroxyl functionalized phenolic compounds makes also quite easy the design and synthesis of benzoxazine precursors bearing free additional phenolic hydroxyl groups. In general, the electron donating groups enhance the thermal stability while the electron withdrawing groups lower the thermal stability, which is in the following order: aryl-NHCOO-aryl < alkyl-NHCOO-aryl < aryl-NHCOO-alkyl < alkyl-NHCOO-alkyl.[41] We thus made an assumption that a hybrid polybenzoxazine-polyurethane vitrimer could be endowed with recyclable abilities under mild conditions than Forman's aliphatic carbamate thanks to the presence of these free phenolic hydroxyl groups. To verify this idea, a biobased benzoxazine monomer was synthesized from tyrosol, dodecylamine, and paraformaldehyde. Tyrosol is a natural phenolic antioxidant present in a variety of natural sources, like olive leaves and argan oil. Its molecular structure shows one hydroxyurethane function in addition to the hydroxyl group of the phenol function. Dodecylamine is synthesized by lauric acid produced from vegetable oil. Furfurylamine is synthesized from furfural, a green platform product derived from agricultural by-products such as corncobs and wheat bran. Further, carbamate bond is generated by the reaction of the free hydroxyl group from hydroxyethane function of tyrosol and hexamethylene diisocyanate (HDI). The so prepared chemical structures have been studied and characterized by nuclear magnetic resonance (NMR) spectroscopy. Their curing and the properties of the resulting biobased polybenzoxazine-polyurethane networks have been determined by Fourier transform infra-red (FTIR), differential scanning calorimetry (DSC) and dynamic mechanical thermal analysis (DMA). Moreover, the ability of this thermosetting polybenzoxazine system to be fully recyclable and reprocessable was evaluated and demonstrated.

2 | EXPERIMENTS AND METHODS

2.1 | Materials

Tyrosol (99%), dodecylamine (99%), paraformaldehyde (95%), and hexamethylene diisocyanate (98%) were purchased from Sigma-Aldrich and used without any further purification.

2.2 | Characterization and measurements

2.2.1 | Nuclear magnetic resonance (NMR)

The ^{1}H NMR spectra were recorded with an NMR spectrometer (Bruker, 500 MHz) at room temperature. Solvent: deuterated chloroform ($CDCl_3$); internal reference: tetramethyl silane (TMS).

2.2.2 | Gel fraction measurements

A piece of sample (W_0 g) was swelled and extracted by chloroform at room temperature for 24 h to remove the un-crosslinking part. The residue was collected and weighed (W_1 g) after drying in vacuo at 60°C for 24 h. The sample was tested three times. The gel fraction (G%) was calculated by the following Equation 1:

$$G\% = w_1/w_0 * 100\%. \quad (1)$$

2.2.3 | Fourier transform infrared spectroscopy (FT-IR)

Precursors and crosslinked polymers were analyzed using a Bruker IFS 66v/S spectrometer to detect the conversions of the benzoxazine ring and furan ring. Spectra were recorded under vacuum from 500 to 4000 cm^{-1} with a wavenumber resolution of 4 cm^{-1}. 64 scans were collected for each sample.

2.2.4 | Differential scanning calorimetry (DSC)

DSC was recorded on a DSC Q200 (TA Instruments, USA) under nitrogen flow of 50 mL min^{-1}, over the temperature ranges 0–300°C with a heating or cooling rate of 10°C min^{-1}.

2.2.5 | Dynamic mechanical analysis (DMA)

Thermomechanical properties of the sample was carried out on DMA Q800 (TA Instruments, USA), with a heating rate of 3°C min^{-1} from room temperature to 300°C and a frequency of 1 Hz.

2.2.6 | Relaxation experiment

The experiments were carried out on DMA with stress relaxation model at varying temperatures from 110 to 170°C. The samples were allowed to equilibrate at special temperature for approximately 5 min, and then were subjected to a constant strain (1%). The characteristic relaxation time (τ*) was defined as the time required for the stress relaxation modulus to reach 37% of its initial value and determined via DMA.

2.2.7 | Tensile stress test

Samples with a dog-bone shape were used for the tensile stress test, using a SANS CMT4104 (SANS Group, China) at a crosshead speed of 3 mm min^{-1} at 25°C. The thickness and width of the samples were kept at 0.5 and 4 mm.

2.3 | Syntheses

2.3.1 | Synthesis of T-Dod

Tyrosol 20 g (0.145 mol) and dodecylamine 26.78 g (0.145 mol) were mixed with a mechanical agitator at 120°C in a long 250 mL beaker until the complete dissolution of tyrosol. Paraformaldehyde, in excess of 10%, 4.78 g (0.159 mol), was then rapidly introduced under vigorous stirring in order to limit the bubbling due to the rapid decomposition of paraformaldehyde into formaldehyde. The mixture was then allowed to react for 25 min under continuous stirring. The crude reaction product was dissolved in 200 mL chloroform, washed with saturated solution of sodium bicarbonate (3*200 mL) and deionized water (200 mL) in a separatory funnel. The combined organic was concentrated under reduced pressure and dried under vacuum at 40°C overnight. White solid T-Dod was obtained, 45 g (weight yield 90%).

2.3.2 | Synthesis of T-HDI-Dod

T-Dod (17.35 g, 0.05 mol) was dissolved in 100 mL dry chloroform at 60°C with N_2. Hexamethylene diisocyanate (4.2 g, 0.025 mol) was dissolved in 50 mL dry chloroform and then added into the solution with DBTDL (0.0005 mmol, 1 mol% to monomer) as catalyst. The mixture was stirred for 3 h. After cooling to room temperature, the mixture was precipitated into methanol and dried under vacuum at 40°C overnight. White solid T-HDI-Dod was obtained, 20 g (weight yield 93%).

2.4 | Curing of T-HDI-Dod resins

All the precursors were introduced in a stainless steel mold (60*12*3 mm), molten, further degassed in a vacuum oven at 140°C for 10 min, and then step cured in an air-circulating oven according to the following cycle: 2 h at 150°C and 2 h at 180°C. Thereafter, samples were allowed to slowly cool down to room temperature before their unmolding.

3 | RESULTS AND DISCUSSION

3.1 | Synthesis of the benzoxazine monomer T-HDI-Dod

The synthetic route for the formation of the benzoxazine monomer T-HDI-Dod is depicted in Scheme 1. First, a fully biobased benzoxazine monomer T-Dod is prepared by condensation reactions of tyrosol, paraformaldehyde, and dodecylamine via a solventless synthesis procedure. Then, carbamate bond was successfully formed by reacting T-Dod and HDI to achieve T-HDI-Dod. A white solid was obtained.

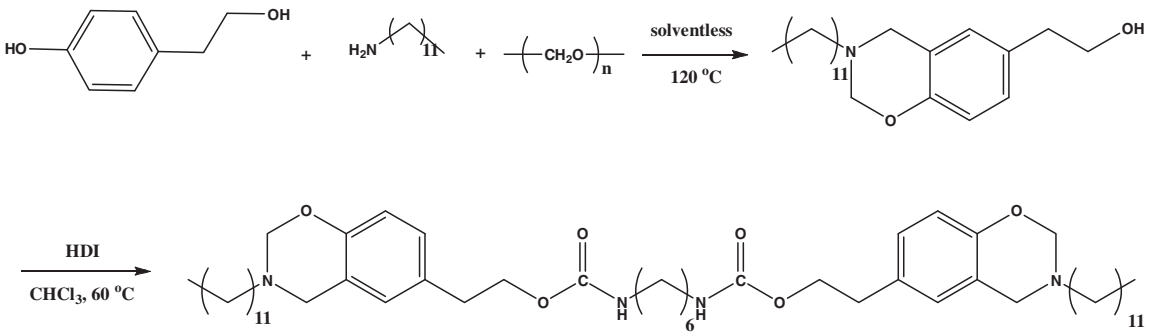

SCHEME 1 Synthesis of the benzoxazine monomer T-HDI-Dod

The structures of synthesized benzoxazine monomers were detected by FTIR as shown in Figure 1. For T-Dod (red line), the characteristic absorption bands of the oxazine ring were indicated by the bands at 1501 cm^{-1} (the trisubstituted benzene ring stretching), 1338 cm^{-1} (the CH_2 wagging into the closed benzoxazine ring), 1232 cm^{-1} (the aromatic C—O—C asymmetric stretching), 1047 cm^{-1} (the asymmetric stretching vibration bands of C—N—C), 1139 cm^{-1} (the C-H in plane vibration), 954 cm^{-1} (the C—H out of plane deformation in the aromatic ring fused to the oxazine ring). O—H stretching vibration and out-of-plane wagging deformation were detected at 3240 and 717 cm^{-1}. For T-HDI-Dod (black line), a characteristic absorption bands of the carbonyl were obtained at 1684 cm^{-1} (the stretching vibration). Moreover, the disappearance of O-H peaks and the appearance of N—H stretching vibration at 3343 cm^{-1} confirm the involvement of carbamate bond.

The structures of synthesized benzoxazine monomers were confirmed by ^{1}H NMR (Figure 2). In detail, the peaks at 4.72 ppm (δH^f) and 3.97 ppm (δH^g) correspond to the characteristic protons of O—CH_2—N and Ar—CH_2—N of the oxazine ring, respectively. The appearance of peaks in the interval δ = 6.55–6.85 ppm is assigned to aromatic protons close to benzoxazine ring. The result confirms the formation of benzoxazine ring. Moreover, the peak of the protons (δH^e) of —CH_2O— shifts from 3.82 ppm to 4.08 ppm as well as the peak at 3.16 ppm (δH^k) caused by the characteristic protons of —CH_2N suggest that T-HDI-Dod has been successfully synthesized.

3.2 | Curing behavior of the precursors

The curing behavior of T-HDI-Dod was characterized by DSC. Two transitions were mainly observed. First, there was a sharp endothermic melting peak that appeared at about 125°C. Second, an exothermic peak with maximum temperature at 254°C was observed and ascribed to ring

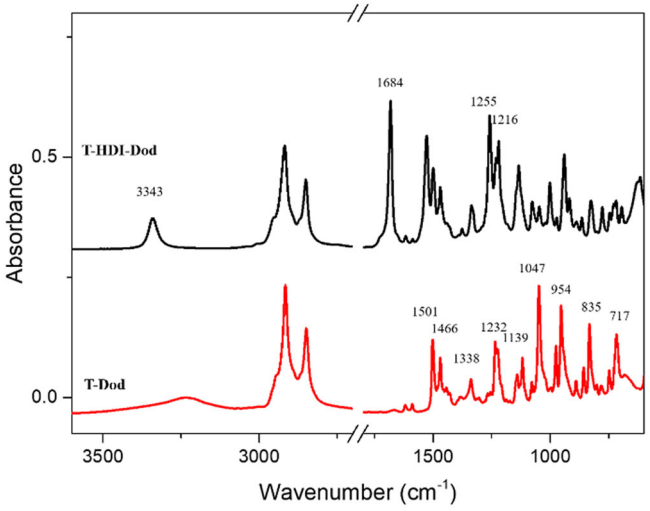

FIGURE 1 The FTIR spectra of T-Dod and T-HDI-Dod [Color figure can be viewed at wileyonlinelibrary.com]

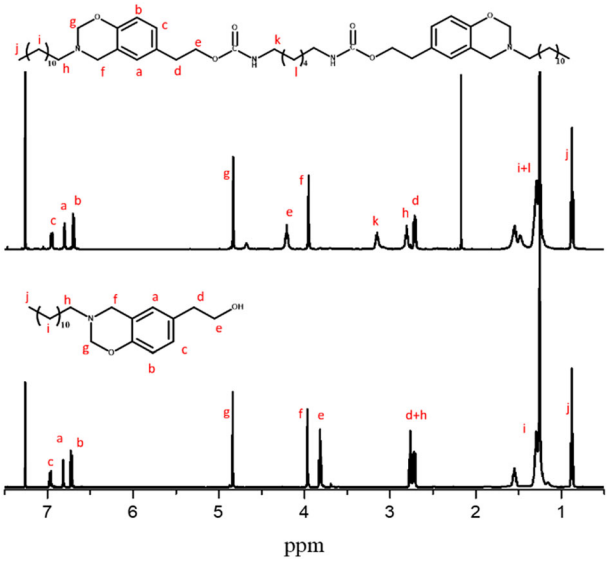

FIGURE 2 ^{1}H NMR spectra of T-Dod and T-HDI-Dod in $CDCl_3$ [Color figure can be viewed at wileyonlinelibrary.com]

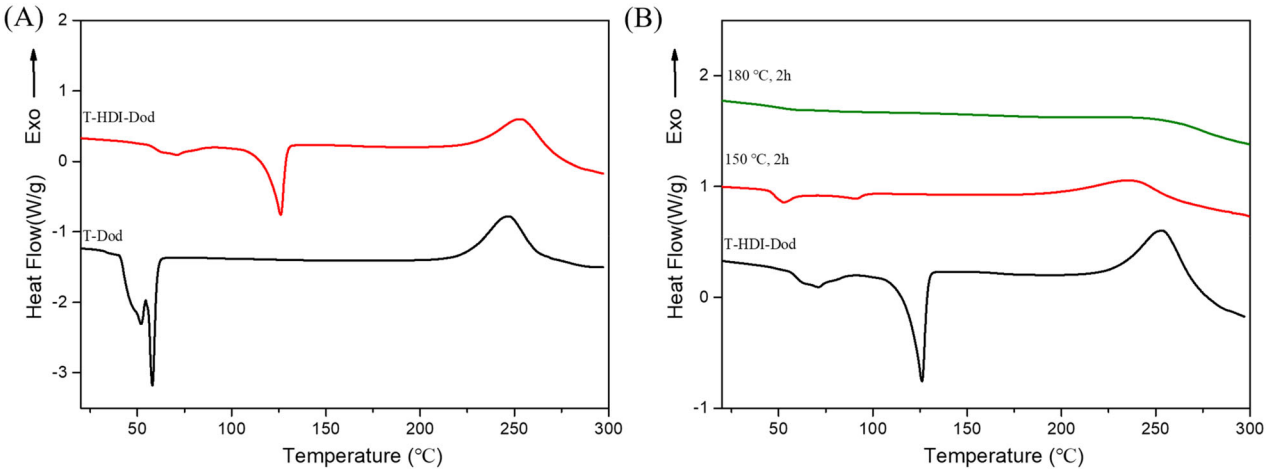

FIGURE 3 (a) DSC heating curves of T-Dod and T-HDI-Dod precursors. (b) DSC heating curves of p(T-HDI-Dod) as recorded after the step by step curing stage (after being cured at 150°C for 2 h and 180°C for 2 h) [Color figure can be viewed at wileyonlinelibrary.com]

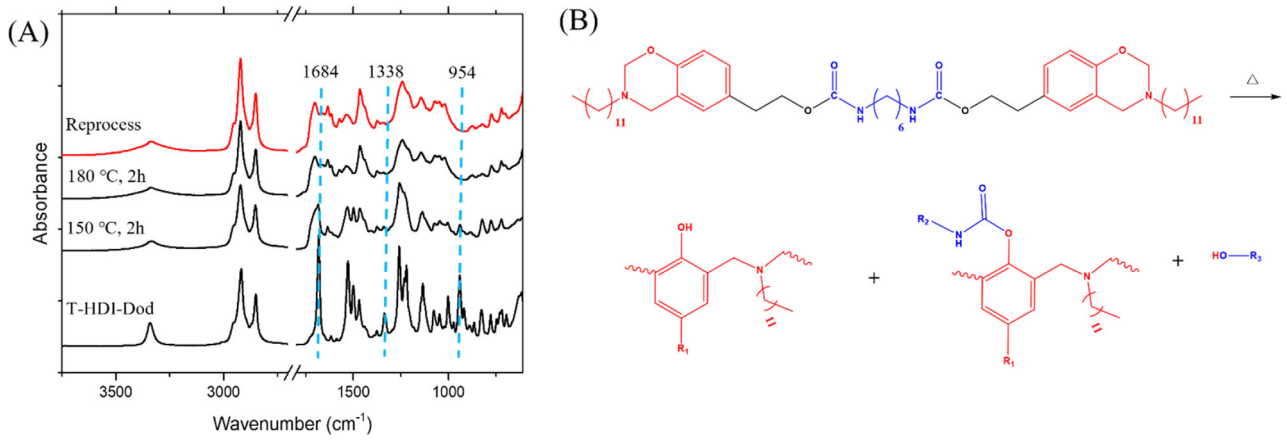

FIGURE 4 (a) The FTIR spectra of T-HDI-Dod during the step by step curing reaction after the step by step curing stage (after being cured at 150 °C for 2 h and 180 °C for 2 h) and the reprocessed p(T-HDI-Dod). (b) Illustration of the possible crosslink and transcarbamate reaction during the curing process [Color figure can be viewed at wileyonlinelibrary.com]

opening polymerization of benzoxazine. It is worth noting that the maximum of ring-opening polymerization temperature of T-HDI-Dod is found to be shifted to higher temperature than the one of T-Dod polymerization (i.e., 254°C instead of 247°C) (Figure 3a). This effect may be explained by the absence of free *p*-substituted hydroxyl groups on T-HDI-Dod precursors when compared to T-Dod ones. Indeed, hydroxyl functions are known to catalyze ring opening polymerization of benzoxazines.[16,42] The value of the exothermic enthalpy is about 78.1 kJ mol^{-1}, which is consistent with 73 kJ mol^{-1} of bisphenol-A based benzoxazine ring recorded by Ishida et al.[43] The result indicates a good polymerization ability.

To further investigate the polymerization process, a controlled step by step curing procedure was established and the enthalpy after each step was determined by DSC. As shown in Figure 3b, it was noted that the exothermic peak associated with the ring opening polymerization is gradually consumed along with the curing process. Finally, the exothermic peak almost disappeared after curing at 180°C for 2 h, indicating the complete curing reaction.

FTIR technology was usually used to monitor the structure evolution and analyze the curing behaviors of benzoxazines during the curing process. The FTIR spectra of T-HDI-Dod at different curing stages are shown in Figure 4. When it was cured step by step, the characteristic signals mainly standing for the oxazine ring at 954 and 1338 cm^{-1} all disappeared, indicating the ring-opening reaction of the benzoxazine monomer. In fact, the exchange reaction of dynamic carbamate exists during the whole curing. The peak in the carbonyl region at aliphatic carbamate at 1684 cm^{-1} will partly move to

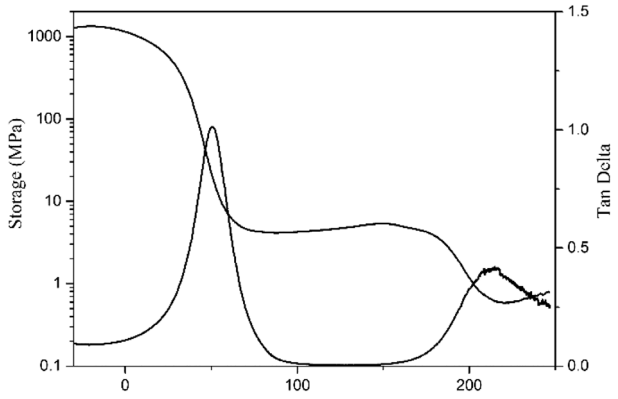

FIGURE 5 Thermomechanical behavior of p(T-HDI-Dod) by DMA analysis

1720 cm^{-1}, corresponding to a phenolic carbamate C=O stretch. The illustration of the possible crosslink and transcarbamate reaction during the curing process has been present in Figure 4b.

3.3 | Thermomechanical behaviors of cured p(T-HDI-Dod)

The thermo-mechanical properties of the cured p(T-HDI-Dod) were investigated by DMA analysis as shown in Figure 5. Two transitions are observed by DMA revealing two distinct phenomena. A first one appears at about 51°C and is attributed to the thermomechanical transition associated to a glass transition of the material, which is agree well with the result observed around 55°C on DSC curves (Figure 3b). Indeed, the storage modulus of the cured p(T-HDI-Dod) system exhibits as expected quite high storage modulus G_0 (1.35 GPa) in the glassy state, that is, below 51°C. Then, at around 51°C, the G_0 declines dramatically with a clear sharp peak observed on the tan δ curve which is characteristic of the glass transition. Interestingly, storage modulus G_0 maintains a rubber plateau above the glass transition temperature relevant of the good formation of a network upon curing. Finally, a second drop of the storage modulus appears at 180°C that is ascribed to the significant dissociation of the carbamate bonds. It is to note that the storage modulus above 180°C still shows a plateau with a lower value evidencing the persistence of the crosslinks due to benzoxazine bonds.

3.4 | Stress relaxation on the carbamate bond

Generally, carbamate bonds are typically "sluggish" and transcarbamoylation often requires very high temperature (>200°C) with unexpected side reactions. Some reported polyurethane networks usually exhibit reprocessable abilities with assistance of catalyst dibutyltin dilaurate.[40,44] Recently a report on polyhydroxyurethane systems demonstrated they represent an effective approach to accelerate transcarbamoylation.[31] The gel fraction of our material is 92.7 ± 2.3% indicating crosslinked network structure. Moreover, our current work is catalyst free and higher crosslinked. Thus, stress relaxation experiments on catalyst-free p(T-HDI-Dod) system were investigated at different temperatures to study its dynamic behavior.[45,46] The elaborated samples were allowed to equilibrate at different temperatures for approximately 5 min, and then were subjected to a constant strain (1%). Figure 6a shows the stress relaxation behaviors determined by DMA at varying temperatures from 110 to 170 °C. Unexpectedly, the stress released fully at 130 °C within 10 min.

The characteristic relaxation time (τ^*) was defined as the time required for the stress relaxation modulus to reach 37% (1/e) of its initial value and determined via DMA. These points were then plotted versus 1000/T (Insert Figure 6a) and fit to the Arrhenius relationship in Equation 2.

$$\tau*(T) = \tau_0 e^{Ea/RT}, \tag{2}$$

where τ_0 is the characteristic relaxation time at infinite T, Ea is the activation energy of the bond exchange reaction (kJ mol^{-1}), R is the universal gas constant (8.314 J K^{-1} mol^{-1}) and T is the temperature (K).

Equation (1) can be transformed to Equation (3):

$$\ln \tau*(T) = \ln \tau_0 + Ea/RT \tag{3}$$

Referring to Figure 6b, Equation (3) for p(T-HDI-Dod) is transformed into Equation (4).

$$\ln \tau*(T) = 11.05*1000/T - 22.6. \tag{4}$$

So the activation energy is 92 kJ mol^{-1}. This relative lower Ea is caused by associative transcarbamoylation reactions with the contribution of hydroxyl groups.

One of the most promising characteristic properties of vitrimers is their recyclability, which is extremely difficult with traditional thermosets. Cutting into many small fragments, the network was shown to be capable of healing and reforming into new, continuous films (Figure 6b) under relatively mild conditions. Small pieces were pressed (10 MPa) and heated (130°C) for 10 min to regenerate an optically transparent film. The FTIR of reprocessable sample has been investigated (Figure 4a).

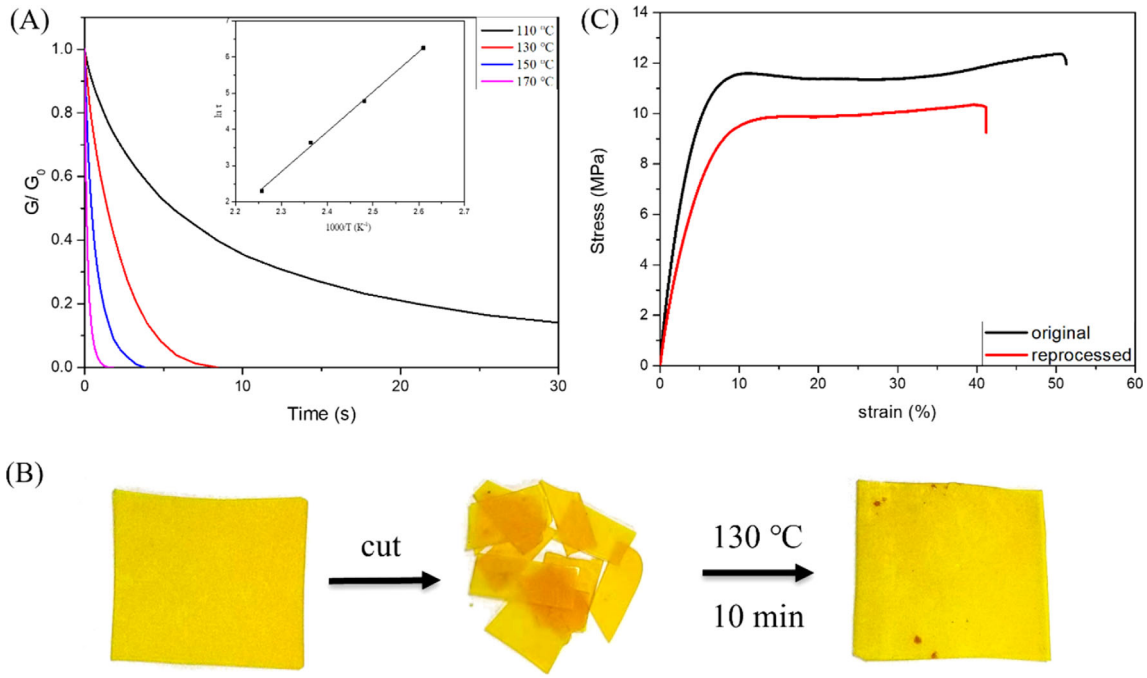

FIGURE 6 (a) Thermal stress relaxation of p(T-HDI-Dod) film at different temperatures with a strain of 1%. G and G0 represent the instantaneous stress and the initial relaxation modulus, respectively. Insert figure: Arrhenius analysis on p(T-HDI-Dod). (b) "cut and regenerate" tests of the elaborated films. (c) Tensile tests of the reprocessed p(T-HDI-Dod) along with the original film [Color figure can be viewed at wileyonlinelibrary.com]

Compared to the cured fresh sample, the reprocessable one has the all same peaks. The result proves our suppose that the dynamic trancarbamate reaction takes place and equals to equilibrium during the whole curing procedure. We also tested the tensile tests of virgin p(T-HDI-Dod) and the reprocessed sample **(**Figure 6c). More than 90% of the tensile strength (from 11.7 to 10.2 MPa) and 80% of strain (from 51% to 41%) of the film was recovered after the complete recycle. The results indicated that the catalyst-free polybenzoxazine-polyurethane network has excellent reprocessable ability.

4 | CONCLUSIONS

In this article, a catalyst-free reprocessable polybenzoxazine-polyurethane thermoset based on thermal dynamic exchange of the carbamate bonds has been developed. The curing characteristics and properties of this biobased polybenzoxazine-polyurethane have been determined by Fourier transform infra-red (FTIR), differential scanning calorimetry (DSC) and dynamic mechanical thermal analysis (DMA). Moreover, the successful tests of the recyclability of the material was achieved at the mild reprocess condition (130°C, 10 min). This work provides a promising potential in industrial applications as a new recyclable and reprocessable thermosetting polybenzoxazine.

ACKNOWLEDGMENTS

The authors wish to thank Wallonie and European Community for general support in the frame of the "Programme d'Excellence FLYCOAT", the INTERREG V program (ATHENS and BIOCOMPAL projects) and the FEDER 2014-2020 program: HYBRITIMESURF, MACOBIO, and BIOMAT projects.

DATA AVAILABILITY STATEMENT

Research data are not shared.

ORCID

Zhibin Wen https://orcid.org/0000-0002-2230-2996

REFERENCES

[1] C. R. Nair, *Prog. Polym. Sci.* **2004**, *29*, 401.
[2] H. Ishida, T. Agag, *Handbook of benzoxazine resins*, Elsevier, Amsterdam **2011**.
[3] N. Ghosh, B. Kiskan, Y. Yagci, *Prog. Polym. Sci.* **2007**, *32*, 1344.
[4] I. R. Nawaz, T. Wang, A. A. K. Gorar, A. G. Soomro, S. K. Sami, A. H. Shah, J. Wang, W. B. Liu, S. H. Sultan, A. A. Babar, *J. Appl. Polym. Sci.* **2021**, *138*, 51279.
[5] P. Thirukumaran, R. Sathiyamoorthi, A. Shakila Parveen, M. Sarojadevi, *Polym. Compos.* **2016**, *37*, 573.

[6] S. Li, T. Zou, L. Feng, X. Liu, M. Tao, *J. Appl. Polym. Sci.* **2013**, *128*, 4164.
[7] A. Van, K. Chiou, H. Ishida, *Polymer* **2014**, *55*, 1443.
[8] X.-L. Zhao, Y.-Y. Liu, Y. Weng, Y.-D. Li, J.-B. Zeng, *ACS Sustainable Chem. Eng.* **2020**, *8*, 15020.
[9] L. Dumas, L. Bonnaud, M. Olivier, M. Poorteman, P. Dubois, *J. Mater. Chem. A* **2015**, *3*, 6012.
[10] J. Dai, S. Yang, N. Teng, Y. Liu, X. Liu, J. Zhu, J. Zhao, *Coatings* **2018**, *8*, 88.
[11] L. Dumas, L. Bonnaud, M. Olivier, M. Poorteman, P. Dubois, *Eur. Polym. J.* **2015**, *67*, 494.
[12] L. Dumas, L. Bonnaud, M. Olivier, M. Poorteman, P. Dubois, *Eur. Polym. J.* **2016**, *81*, 337.
[13] C. Wang, J. Sun, X. Liu, A. Sudo, T. Endo, *Green Chem.* **2012**, *14*, 2799.
[14] M. L. Salum, D. Iguchi, C. R. Arza, L. Han, H. Ishida, P. Froimowicz, *ACS Sustainable Chem. Eng.* **2018**, *6*, 13096.
[15] C. R. Arza, P. Froimowicz, H. Ishida, *RSC Adv.* **2015**, *5*, 97855.
[16] L. Dumas, L. Bonnaud, M. Olivier, M. Poorteman, P. Dubois, *Green Chem.* **2016**, *18*, 4954.
[17] H. Xu, W. Zhang, Z. Lu, G. Zhang, *RSC Adv.* **2013**, *3*, 3677.
[18] L. R. V. Kotzebue, J. R. de Oliveira, J. B. da Silva, S. E. Mazzetto, H. Ishida, D. Lomonaco, *ACS Sustainable Chem. Eng.* **2018**, *6*, 5485.
[19] L. Bonnaud, B. Chollet, L. Dumas, A. A. Peru, A. L. Flourat, F. Allais, P. Dubois, *Macromol. Chem. Phys.* **2019**, *220*, 1800312.
[20] Z. Wen, L. Bonnaud, R. Mincheva, P. Dubois, J. M. Raquez, *Materials* **2021**, *14*, 440.
[21] D. Montarnal, M. Capelot, F. Tournilhac, L. Leibler, *Science* **2011**, *334*, 965.
[22] C. J. Kloxin, C. N. Bowman, *Chem. Soc. Rev.* **2013**, *42*, 7161.
[23] T. J. White, D. J. Broer, *Nat. Mater.* **2015**, *14*, 1087.
[24] Ž. Štirn, A. Ručigaj, M. Krajnc, *Express Polym. Lett.* **2016**, *10*, 10.
[25] C. I. Chou, Y. L. Liu, *J. Polym. Sci., Part A: Polym. Chem.* **2008**, *46*, 6509.
[26] J.-H. Chen, D. D. Hu, Y. D. Li, J. Zhu, A. K. Du, J. B. Zeng, *Polym. Test.* **2018**, *70*, 174.
[27] F. Fu, M. Huang, W. Zhang, Y. Zhao, X. Liu, *Sci. Rep.* **2018**, *8*, 1.
[28] Y. Yin, J. Yang, L. Meng, *J. Appl. Polym. Sci.* **2021**, *138*, 51010.
[29] N. Zheng, J. Hou, Y. Xu, Z. Fang, W. Zou, Q. Zhao, T. Xie, *ACS Macro Lett.* **2017**, *6*, 326.
[30] Z. B. Wen, R. F. Shao, J. M. Raquez, N. A. Clark, K. K. Yang, Y. Z. Wang, *Sci. China Mater.* **2020**, *63*, 2590.
[31] D. J. Fortman, J. P. Brutman, C. J. Cramer, M. A. Hillmyer, W. R. Dichtel, *J. Am. Chem. Soc.* **2015**, *137*, 14019.
[32] L. Q. Li, X. Chen, J. M. Torkelson, *Macromolecules* **2019**, *52*, 8207.
[33] C. J. Fan, Z. B. Wen, Z. Y. Xu, Y. Xiao, D. Wu, K. K. Yang, Y. Z. Wang, *Macromolecules* **2020**, *53*, 4284.
[34] Z. B. Wen, X. Han, B. D. Fairbanks, K. K. Yang, C. N. Bowman, *Polymer* **2020**, *202*, 122715.
[35] M. Arslan, B. Kiskan, Y. Yagci, *Sci. Rep.* **2017**, *7*, 5207.
[36] M. Arslan, B. Kiskan, Y. Yagci, *Macromolecules* **2018**, *51*, 10095.
[37] A. Adjaoud, A. Trejo-Machin, L. Puchot, P. Verge, *Polym. Chem* **2021**, *12*, 3276.
[38] P. Krol, *Prog. Mater. Sci.* **2007**, *52*, 915.
[39] Y. Camberlin, J. P. Pascault, J. M. Letoffe, P. Claudy, *J. Polym. Sci., Part A: Polym. Chem.* **1982**, *20*, 383.
[40] Z. Wen, M. K. McBride, X. Zhang, X. Han, A. M. Martinez, R. Shao, C. Zhu, R. Visvanathan, N. A. Clark, Y. Wang, K. Yang, C. N. Bowman, *Macromolecules* **2018**, *51*, 5812.
[41] P. I. Kordomenos, J. E. Kresta, *Macromolecules* **1981**, *14*, 1434.
[42] M. Baqar, T. Agag, R. Huang, J. O. Maia, S. Qutubuddin, H. Ishida, *Macromolecules* **2012**, *45*, 8119.
[43] H. Ishida, Y. Rodriguez, *Polymer* **1995**, *36*, 3151.
[44] N. Zheng, Z. Fang, W. Zou, Q. Zhao, T. Xie, *Angew. Chem., Int. Ed.* **2016**, *55*, 11421.
[45] M. Capelot, M. M. Unterlass, F. Tournilhac, L. Leibler, *ACS Macro Lett.* **2012**, *1*, 789.
[46] J. P. Brutman, P. A. Delgado, M. A. Hillmyer, *ACS Macro Lett.* **2014**, *3*, 607.

How to cite this article: Z. Wen, L. Bonnaud, P. Dubois, J.-M. Raquez, *J. Appl. Polym. Sci.* **2022**, *139*(19), e52120. https://doi.org/10.1002/app.52120